

Figure 7. ESR spectrum of doubly oxidized (OEP)Ge(Fc)₂ at 115 K in PhCN, 0.2 M TBAP.

Thus, the final species in solution may be assigned as [(OEP)Ge(Fc)ClO₄]⁺ resulting from the cleavage of one germanium-phenyl bond. Finally, a porphyrin π cation radical is formed after abstraction of one electron from the proposed [(OEP)Ge(Fc)ClO₄]⁺ complex (see Figure 6c). Oxidized (TPP)Ge(C₆H₅)(Fc) shows similar spectroelectrochemical changes, and these spectral data are summarized in Table V.

Reduction of (OEP)Ge(C₆H₅)(Fc) and (TPP)Ge(C₆H₅)(Fc). (OEP)Ge(C₆H₅)(Fc) is reduced at a potential 50 mV positive of (OEP)Ge(Fc)₂ (see Figure 4), but the half-wave potentials for reduction of (TPP)Ge(C₆H₅)(Fc) and (TPP)Ge(Fc)₂ are identical within experimental error (Table IV). Time-resolved thin-layer spectra obtained during reduction of (OEP)Ge(C₆H₅)(Fc) follow the trends for formation of a π anion radical.^{11,12} These spectral changes are shown in Figure 5b. The Soret band at 443 nm and a Q-band at 569 nm disappear after addition of one electron to the complex while new peaks appear at 465, 641, 732, and 846 nm. Four well-defined isosbestic points are present, indicating that only two species, (OEP)Ge(C₆H₅)(Fc) and [(OEP)Ge(C₆H₅)(Fc)]⁻, are in equilibrium. Similar electronic absorption spectral changes are obtained upon reduction of (TPP)Ge(C₆H₅)(Fc), and these data are summarized in Table V.

ESR Spectra of Oxidized (OEP)Ge(Fc)₂ in PhCN, 0.2 M TBAP. No ESR signal is detected after exhaustive bulk electrolysis of (OEP)Ge(Fc)₂ at +0.21 V. This is presumably due to the interaction between the oxidized ferrocenyl group and the porphyrin π ring system. However, an anisotropic ESR spectrum is obtained after controlled-potential electrolysis at 0.42 V (the second oxidation). This signal is shown in Figure 7 and is characterized by $g_{\perp} = 2.054$ and $g_{\parallel} = 2.017$. It is worth noting that this spectrum shows some features similar to those of singly oxidized biferrocenylene,¹³ [Fe₂(C₅H₄)₄]⁺, where the unpaired electron is rapidly exchanging between the two iron centers.¹⁴

Comparisons may be made between the ESR spectrum of [(OEP)Ge(Fc)₂]²⁺ and that of the ferrocenium cation or singly oxidized biferrocenylene.¹³ No downfield absorption band ($g = 3.20$ – 4.35) is observed for the ferrocenium cation in [(OEP)Ge(Fc)₂]²⁺. This might suggest that the charge on a ferrocenyl ligand is less than unity. The similarity in shape of the ESR spectrum for [(OEP)Ge(Fc)₂]²⁺ to that of the upfield absorption band of the singly oxidized biferrocenylene might be additional evidence for a rapid exchange of the electron between the two iron atoms of the oxidized metalloporphyrin.

Comparison of (P)Ge(Fc)₂ and (P)Ge(C₆H₅)(Fc) with Other (P)Ge(R)₂ Complexes. The (P)Ge(C₆H₅)(Fc) complexes provide the first synthetic examples of metalloporphyrins containing two different metal-carbon- σ -bonded axial groups. The physico-

chemical properties of neutral (P)Ge(Fc)₂ and (P)Ge(C₆H₅)(Fc) are similar to other σ -bonded (P)Ge(R)₂ complexes. However, the Fc complexes show an additional unique feature. The Soret band molar absorptivities of (P)Ge(Fc)₂ and (P)Ge(C₆H₅)(Fc) are only about half those of other (P)Ge(R)₂ complexes (see Table I), and this can be unambiguously attributed to a delocalization of electron density from the porphyrin macrocycle onto the ferrocenyl group. As a consequence, the germanium-carbon σ -bonds in (P)Ge(Fc)₂ and (P)Ge(C₆H₅)(Fc) are much more stable than the metal-carbon bonds in other (P)Ge(R)₂ complexes.

The enhanced stability of [(P)Ge(C₆H₅)(Fc)]⁺ with respect to the highly reactive [(P)Ge(C₆H₅)₂]⁺ complex⁵ results from delocalization of positive charge onto the porphyrin macrocycle. This delocalization effect (with respect to Fc⁺/Fc) amounts to -180 mV for [(TPP)Ge(C₆H₅)(Fc)]⁺ and -250 mV for [(OEP)Ge(C₆H₅)(Fc)]⁺. For [(P)Ge(Fc)₂]⁺ both a delocalization of positive charge onto the porphyrin macrocycle and an interaction between two iron centers results in greater stabilization. The overall effect with respect to Fc⁺/Fc in PhCN is -250 mV for [(TPP)Ge(Fc)₂]⁺ and -330 mV for [(OEP)Ge(Fc)₂]⁺.

On the other hand, the stability of the metal-carbon σ -bond in the dialkyl- or diarylgermanium(IV) porphyrins of the form (P)Ge(R)₂ can be varied with changes in the degree of electron donation by the axial ligand.⁵ The more electron-withdrawing the R group, the more stable the σ -bond will be and the more positive the first oxidation potential will be. An anodic shift of about 240 mV was observed between the first oxidation peak potential of the (P)Ge(R)₂ complex containing the strongest σ -bonding R group (R = C₆H₅) and that containing the weakest σ -bonding ligand (R = CH₂C₆H₅).⁵

Finally, differences between the stability of [(P)Ge(Fc)₂]⁺ or [(P)Ge(C₆H₅)(Fc)]⁺ and other [(P)Ge(R)₂]⁺ complexes are also related to a difference in the site of oxidation between the two types of complexes. For the former two series of complexes the site of the initial electrooxidation is clearly at the axial ligand position, but this is unclear for the other σ -bonded (P)Ge(R)₂ complexes.

Acknowledgment. The support of the National Science Foundation (Grant No. 8515411) is gratefully acknowledged.

Registry No. (OEP)Ge(Fc)₂, 109335-07-1; (OEP)Ge(C₆H₅)Fc, 114467-16-2; (TPP)Ge(C₆H₅)₂, 110718-65-5; (TPP)Ge(C₆H₅)Fc, 114467-17-3; (TPP)Ge(Fc)₂, 11060-95-0; (OEP)GeCl₂, 31713-45-8; (OEP)Ge(C₆H₅)Cl, 110718-66-6; (TPP)GeCl₂, 41043-38-3; (TPP)Ge(C₆H₅)Cl, 111237-13-9; (OEP)Ge(C₆H₅)₂, 110718-63-3; [(TPP)Ge(Fc)₂]⁻, 114594-51-3; [(TPP)Ge(Fc)₂]²⁻, 114594-52-4; [(OEP)Ge(C₆H₅)(Fc)]⁺, 114674-33-8; [(TPP)Ge(Fc)₂]⁺, 114594-53-5; [(TPP)Ge(C₆H₅)(Fc)]⁺, 114614-03-8; [(OEP)Ge(C₆H₅)(Fc)]⁻, 114594-54-6.

Contribution from the Department of Chemistry and Biochemistry, University of Colorado, Boulder, Colorado 80309

Synthesis and Borane Coordination of Primary Alkenyl- and Alkynylphosphines

Robert H. Shay, Bruce N. Diel, David M. Schubert, and Arlan D. Norman*

Received March 14, 1988

Primary alkenyl- and alkynylphosphines are interesting because they contain, in addition to P(III), \geq P donor, and P-H functionalities, carbon-carbon double and triple bonds. Although these compounds offer considerable potential for organophosphine ligand and extended molecule (oligomer/polymer) synthesis, only HC \equiv CPh₂,¹ MeC(PH₂)=CH₂,² PhCH=CHPh₂,³ and CH₂=

(13) Morrison, W. H., Jr.; Krogsrud, S.; Hendrickson, D. N. *Inorg. Chem.* 1973, 12, 1998.

(14) Prins, R. *Mol. Phys.* 1970, 19, 603.

* To whom correspondence should be addressed.

Table I. Infrared Absorptions (cm^{-1}) for $\text{CH}_2=\text{CHCH}_2\text{PH}_2$ (1), $\text{CH}_2=\text{CHCH}_2\text{CH}_2\text{PH}_2$ (2), and $\text{HC}\equiv\text{CCH}_2\text{PH}_2$ (3)

1 ^{a,b}	2 ^b	3 ^b
3090 s	3090 s	3335 vs
2984 m	2990 s	2933 w
2916 m	2928 s	2301 vs
2290 vs	2850 m	2129 m
1818 w	2303 vs	1418 w
1633 s	1648 m	1257 s
1419 w	1642 m	1243 s
1198 w	1440 m	1230 sh
1080 s	1087 s	1095 sh
979 m	994 s	1083 m
942 sh	918 s	943 m
902 vs		863 m
840 m		848 m
675 vs		833 sh
578 m		628 vs
		432 m

^a Abbreviations: vs, very strong; s, strong; m, medium; w, weak; sh, shoulder. ^b Gaseous sample in KBr window cells.

CHCH_2PH_2 have been reported. Further, all were obtained in relatively inefficient syntheses. Thus, it is possible that the effective development of primary alkenyl- and alkynylphosphine chemistry might depend on the availability of a viable synthetic method.

Previous work in our laboratories has established that $\text{LiAl}(\text{PH}_2)_4$ is a highly effective phosphinating agent for the preparation of functionally reactive phosphinosilanes, -germanes, and -stannanes.⁵⁻⁸ In some cases, phosphines can be obtained that appear to be otherwise not available,^{6,7} indicating that $\text{LiAl}(\text{PH}_2)_4$ is a mild and selective phosphinating reagent. Except for $\text{C}_2\text{H}_5\text{PH}_2$ synthesis in the initial report of $\text{LiAl}(\text{PH}_2)_4$,⁹ use of the latter for organophosphine synthesis has not been studied. We have now completed a study of this reagent for the synthesis of primary alkenyl- and alkynylphosphines. Our results are described below.

Experimental Section

Apparatus and Materials. All manipulations were carried out with standard high-vacuum apparatus.¹⁰ Mass spectra were obtained on Varian MAT CH-5 and CH-7 spectrometers. All data were obtained at an ionizing voltage of 70 eV. Infrared spectra were recorded with Perkin-Elmer Model 337G and Beckman 467 and IR 4250 spectrometers on gaseous samples in 10-cm KBr window cells. Proton NMR spectra were obtained at 60.0 and 100.0 MHz on Varian EM-360 and JEOL-PFT 100 spectrometers, respectively. ¹¹B NMR spectra were obtained at 32.1 MHz on a Varian HA-100 spectrometer. ³¹P and ¹³C NMR spectra were obtained on the PFT-100 spectrometer at 40.5 and 25.1 MHz with the use of standard ³¹P and ¹³C probe accessories. ³¹P, ¹³C, ¹H, and ¹¹B chemical shifts are reported relative to 85% H_3PO_4 , Me_4Si , Me_4Si , and $\text{BF}_3\cdot\text{OEt}_2$, respectively. Shifts downfield from the standards are given positive (+ δ) values. NMR spectral simulations were carried out with the Nicolet 1083 Data System and NMRCAL simulation program.

The $\text{LiAl}(\text{PH}_2)_4$ solutions⁵⁻⁸ and B_2H_6 ¹¹ were prepared as described previously. Vinyl bromide ($\text{CH}_2=\text{CHBr}$), $\text{CH}_2=\text{CHCH}_2\text{Cl}$, $\text{CH}_2=\text{C}(\text{H})\text{CH}_2\text{Br}$, $\text{CH}_2=\text{CHCH}_2\text{CH}_2\text{Br}$, and $\text{HC}\equiv\text{CCH}_2\text{Br}$ (Aldrich Chemicals) were distilled before use.

Synthesis of $\text{CH}_2=\text{CHCH}_2\text{PH}_2$ (1), $\text{CH}_2=\text{CHCH}_2\text{CH}_2\text{PH}_2$ (2), and $\text{HC}\equiv\text{CCH}_2\text{PH}_2$ (3). Typically, $\text{CH}_2=\text{CHCH}_2\text{X}$ (X = Cl, Br), $\text{CH}_2=\text{C}(\text{H})\text{CH}_2\text{X}$ (X = Cl, Br), or $\text{HC}\equiv\text{CCH}_2\text{X}$ (X = Cl, Br) were reacted with $\text{LiAl}(\text{PH}_2)_4$ in triglyme.

Table II. NMR Spectral Parameters for $\text{CH}_2=\text{CHCH}_2\text{PH}_2$ (1), $\text{CH}_2=\text{CHCH}_2\text{CH}_2\text{PH}_2$ (2), and $\text{HC}\equiv\text{CCH}_2\text{PH}_2$ (3)

	(a)H H-C=C (b)	H(c) C=C (d) CH ₂ PH ₂ (f)	(a)H H-C=C (b)	H(c) C=C (d) CH ₂ CH ₂ PH ₂ (e) (f)	HC≡CCH ₂ PH ₂ (a) (d) (f)
³¹ P NMR Spectrum ^a					
δ	-132.6 (t) ^b		-140.5 (t)		-130.4 (t)
¹ J(P-H), Hz	195.0		187.7		188.0
¹³ C NMR Spectrum ^c					
$\delta(\text{C}_1)$	18.9 (d) J = 9.8 Hz		37.0 (d) J = 3.7 Hz		2.8 (d) J = 11.0 Hz
$\delta(\text{C}_2)$	114.8 (d) J = 6.1 Hz		13.3 (d) J = 9.8 Hz		69.6 (s)
$\delta(\text{C}_3)$	138.8 (s)		138.1 (d) J = 6.1 Hz		84.3 (s)
$\delta(\text{C}_4)$			114.9		
¹ H NMR Spectrum ^{d,e}					
$\delta(\text{H}_a)$	4.90 (c, a1)		4.90		2.09 (c, a1)
$\delta(\text{H}_b)$	4.96 (c, a1)				
$\delta(\text{H}_c)$	5.90 (c, a1)		5.7		
$\delta(\text{H}_d)$	1.94 (d, a2)		2.1 (q, a2)		2.34 (c, a2)
$\delta(\text{H}_e)$			1.4 (q, a2)		
$\delta(\text{H}_f)$	2.62 (d, a2)		2.60 (d, a2)		3.09 (d, a2)

^a 10% by volume in CDCl_3 . ^b Abbreviations: t = triplet, d = doublet, s = singlet, q = quintet, and c = complex. ^c ¹H decoupled; 10% by volume in C_6D_6 . ^d 15g by volume in C_6D_6 . ^e Complete J data for 1 and 3 in text.

$\text{CHCH}_2\text{CH}_2\text{Br}$, or $\text{HC}\equiv\text{CCH}_2\text{Br}$ (20–22 mmol) in triglyme was allowed to react at 0 °C with $\text{LiAl}(\text{PH}_2)_4$ (7.1–8.0 mmol). After 1.75–4.0 h, the reaction mixture was warmed to ambient temperature. Volatile components were removed in vacuo and separated by low-temperature high-vacuum fractional distillation. From their respective reactions, $\text{CH}_2=\text{CHCH}_2\text{PH}_2$ (1), $\text{CH}_2=\text{CHCH}_2\text{CH}_2\text{PH}_2$ (2), and $\text{HC}\equiv\text{CCH}_2\text{PH}_2$ (3) were obtained in 55–68% yields. $\text{CH}_2=\text{CHCH}_2\text{PH}_2$ was obtained in pure form and in highest yield from $\text{LiAl}(\text{PH}_2)_4/\text{CH}_2=\text{CHCH}_2\text{Br}$ reactions since it is easier to separate $\text{CH}_2=\text{CHCH}_2\text{PH}_2$ from $\text{CH}_2=\text{CHCH}_2\text{Br}$ than from $\text{CH}_2=\text{CHCH}_2\text{Cl}$. ³¹P NMR spectra of the distillation fractions which preceded $\text{CH}_2=\text{CHCH}_2\text{PH}_2$ off the column exhibited primary phosphine triplet resonances at δ -162 (MePH_2)¹² and δ -128 and -145 (possibly due to $\text{CH}_3\text{C}(\text{PH}_2)=\text{CH}_2$ and $\text{CH}_2=\text{C}=\text{CH}(\text{PH}_2)$).

$\text{CH}_2=\text{CHBr}$ with $\text{LiAl}(\text{PH}_2)_4$ in triglyme underwent no reaction after 14 h at 25 °C.

Characterization Data for 1–3. Analyses. Calcd for 1, $\text{C}_3\text{H}_5\text{P}$: 48.65; H, 9.53; P, 41.82. Found: C, 48.80; H, 9.45; P, 41.65. Calcd for 2, $\text{C}_4\text{H}_7\text{P}$: C, 54.54; H, 10.30. Found: C, 54.70; H, 10.21. Calcd for 3, $\text{C}_3\text{H}_3\text{P}$: C, 50.01; H, 7.00. Found: C, 50.11; H, 6.78.

IR data are tabulated in Table I.

NMR Data (¹H, ³¹P, and ¹³C). Chemical shift and selected coupling constant data are given in Table II. Proton coupling constants for 1 and 3 were analyzed in detail by using a combination of spectral simulation techniques and homonuclear (¹H) and heteronuclear (³¹P) spin decoupling. Coupling constants are as follows [referred to by notation used in Table II (J, Hz)]. For 1: H_a-H_b (1.8), H_a-H_c (10.2), H_a-H_d (1.4), H_b-H_c (17.3), H_b-H_d (1.3), H_c-H_d (7.3), H_d-H_f (7.2), P- H_a (2.0), P- H_b (2.0), P- H_c (4.2), P- H_d (7.6). For 3, H_a-H_d (2.7), H_d-H_f (7.4). Coupling constants for 2 were not analyzed in detail owing to spin limitations in the NMRCAL simulation program.

MS Data. The most intense peak in the parent and four most intense ion envelopes are as follows [m/e (relative intensities)]: 1: 74 (100), 57 (22), 45 (28), 41 (97), 39 (58). 2: 88 (70), 60 (100), 55 (87), 47 (62), 39 (79). 3: 72 (36), 69 (43), 57 (100), 45 (25), 39 (45).

Vapor Pressures. Selected values are as follows [temp, °C (P_{Torr})]: 1: -63.5 (1.15), -39.7 (8.90), -19.7 (32.65), 0.0 (95.60). 2: -21.0 (5.00), -8.0 (11.50), 0.0 (18.60), 22.2 (62.20). 3: -45.0 (1.60), -27.0 (6.55), -15.1 (14.85), 0.0 (37.65).

Vapor Pressure Thermodynamic Data. 1: $\log P_{\text{Torr}} = 8.251 - 1.709 \times 10^3/T$, extrapolated bp(760 Torr) = 45.0 °C, $\Delta H_{\text{vap}} = 32.72$ kJ/mol, $\Delta S_{\text{vap}} = 102.9$ J/(mol-deg). 2: $\log P_{\text{Torr}} = 7.869 - 1.802 \times 10^3/T$, extrapolated bp(760 Torr) = 88.1 °C, $\Delta H_{\text{vap}} = 34.52$ kJ/mol, $\Delta S_{\text{vap}} = 95.4$ J/(mol-deg). 3: $\log P_{\text{Torr}} = 8.624 - 1.923 \times 10^3/T$, extrapolated bp(760 Torr) = 61.6 °C, $\Delta H_{\text{vap}} = 36.22$ kJ/mol, $\Delta S_{\text{vap}} = 110.0$ J/(mol-deg).

- Albrand, J. P.; Anderson, S. P.; Goldwhite, H.; Huff, L. *Inorg. Chem.* **1975**, *14*, 570.
- Goldwhite, H. *J. Chem. Soc. A* **1965**, 3901.
- (a) Bogolyubov, G. M.; Petrov, A. A. *Zh. Obshch. Khim.* **1963**, *33*, 3774. (b) Ionin, B. I.; Bogolyubov, G.; Petrov, A. A. *Russ. Chem. Rev. (Engl. Transl.)* **1967**, *36*, 249.
- Chau, S.; Goldwhite, H.; Keyzer, H.; Rosewell, D. G.; Tang, R. *Tetrahedron* **1969**, *25*, 1097.
- Wingeleth, D. C.; Norman, A. D. *Chem. Commun.* **1968**, 812.
- Norman, A. D. *J. Am. Chem. Soc.* **1968**, *90*, 6556.
- Norman, A. D.; Wingeleth, D. C. *Inorg. Chem.* **1970**, *9*, 98.
- Norman, A. D. *J. Organomet. Chem.* **1971**, *28*, 81.
- Finholt, A. E.; Helling, C.; Imhof, V.; Nielsen, L.; Jacobsen, E. *Inorg. Chem.* **1963**, *2*, 504.
- Shriver, D. F.; Drezdson, M. A. *The Manipulation of Air-Sensitive Compounds*, 2nd ed.; Wiley-Interscience: New York, 1986.
- Norman, A. D.; Jolly, W. L. *Inorg. Synth.* **1968**, *11*, 15.

- Crutchfield, M. M.; Dungan, C. H.; Letcher, J. H.; Mark, V.; Van Wazer, J. R. *Top. Phosphorus Chem.* **1967**, *5*.

Table III. NMR Spectral Data for $\text{CH}_2=\text{CHCH}_2\text{PH}_2\cdot\text{BH}_3$ (**4**) and $\text{HC}\equiv\text{CCH}_2\text{PH}_2\cdot\text{BH}_3$ (**5**)

	$\begin{array}{c} \text{(a)H} \\ \\ \text{H}-\text{C}=\text{C}-\text{H} \\ \quad \\ \text{(b)} \quad \text{(c)} \\ \text{CH}_2\text{PH}_2\cdot\text{BH}_3 \\ \text{(d)} \quad \text{(f)} \quad \text{(g)} \end{array}$	$\begin{array}{c} \text{HC}\equiv\text{CCH}_2\text{PH}_2\cdot\text{BH}_3 \\ \text{(a)} \quad \text{(d)} \quad \text{(f)} \quad \text{(g)} \end{array}$
³¹P NMR Spectrum^a		
δ	-48.2 (t) ^b	-41.7 (t)
$^1J(\text{P-H})$, Hz	375	382
¹¹B NMR Spectrum^a		
δ	-42.4	-41.3
$J(\text{B-P})$, Hz	36.7	30.8
$J(\text{B-H})$, Hz	99.7	100.9
¹H NMR Spectrum^{d,e}		
$\delta(\text{H}_a)$	5.28 (c, a1)	1.50 (c, a1) ^c
$\delta(\text{H}_b)$	5.23 (c, a1)	
$\delta(\text{H}_c)$	5.83 (c, a1)	
$\delta(\text{H}_d)$	2.70 (c, a2)	1.96 (c, a2) ^c
$\delta(\text{H}_f)$	4.54 (sextet, a2)	4.05 (sextet, a2) ^d
$\delta(\text{H}_g)$	0.61 (q, a3)	0.26 (c, a3) ^e

^a 10% by volume in CDCl_3 . ^b For abbreviations, see Table II. ^c From $^1\text{H}\{^{31}\text{P}\}$ NMR spectrum; ^d $J(\text{H-H}) = 3.0$ Hz. ^d From $^1\text{H}\{^{31}\text{P}\}$ NMR spectrum; ^e $J(\text{H-H}) = 7.4$ Hz. ^e From $^1\text{H}\{^{11}\text{B}\}$ NMR spectrum; ^f $J(\text{H-P}) = 16.5$ Hz, ^g $J(\text{H-H}) = 7.4$ Hz.

Thermolyses. (A) $\text{CH}_2=\text{CHCH}_2\text{PH}_2$. Allylphosphine (2.10 mmol) was heated to 105 °C in a sealed 100-mL bulb. The sample was entirely in the gaseous phase. After 21 h, a light yellow film covered the inner surface of the bulb. After 5 days at 100–110 °C, the solid on the walls had increased. Volatile reaction materials were removed and separated by low temperature distillation and found to consist of $\text{CH}_2=\text{CHCH}_3$ (0.05 mmol), unreacted $\text{CH}_2=\text{CHCH}_2\text{PH}_2$ (1.94 mmol), and traces of PH_3 .

(B) $\text{HC}\equiv\text{CCH}_2\text{PH}_2$. $\text{HC}\equiv\text{CCH}_2\text{PH}_2$ (1.99 mmol) in a 500-mL bulb was heated at 105 °C. The sample was entirely in the gas phase. After 3 days, a thin yellow film covered the bulb inner wall. Further heating at 185–195 °C for 23 h produced additional solid in the flask. Removal and separation of volatile reaction materials yielded PH_3 (1.56 mmol) and unreacted $\text{HC}\equiv\text{CCH}_2\text{PH}_2$ (0.42 mmol).

$\text{CH}_2=\text{CCH}_2\text{PH}_2$ and $\text{HC}\equiv\text{CCH}_2\text{PH}_2$ with B_2H_6 . Reactions were carried out in 50-mL bulbs to which a side arm U-tube fitted with an NMR tube or a mass spectral sampling tube was attached. In general, 1 or 3 (0.10–0.34 mmol) and an approximately equimolar amount of B_2H_6 were condensed at -196 °C into the bulb. Reactants were allowed to warm to temperatures ranging from -78 to -45 °C. After 1–3 h, the contents were warmed to 0 °C. Volatile reaction materials were passed through the reactor side arm cooled to -45 °C, through a -130 °C trap, and into a -196 °C trap. No noncondensable gases were observed. Excess B_2H_6 (confirmed by IR spectrum)¹¹ condensed in the -196 °C trap. On the basis of the ratios of 1 and of 3 to B_2H_6 consumed, $\text{CH}_2=\text{CHCH}_2\text{PH}_2\cdot\text{BH}_3$ (**4**) and $\text{HC}\equiv\text{CCH}_2\text{PH}_2\cdot\text{BH}_3$ (**5**) adducts in the ratios 1.00:(0.95–1.05) and 1.00:(0.92–1.03), respectively, were obtained. **4** and **5** are low-volatility, thermally unstable liquids, which distilled slowly into the -45 °C side arm, from which samples for NMR and mass spectral analysis were obtained.

4 and **5** react slowly at 0 °C with additional B_2H_6 . Product mixtures were complex and were not analyzed in detail.

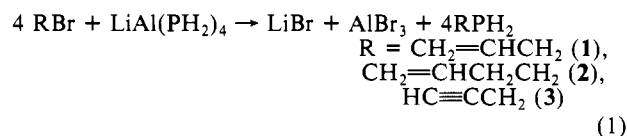
Compounds **4** and **5** undergo slow decomposition above 25 and 0 °C, respectively. After 5 h at 95 °C, **4** becomes completely nonvolatile and intractable. **5** decomposes rapidly at 0 °C to an intractable resin and traces of $\text{CH}_2=\text{CHCH}_2\text{PH}_2$ and PH_3BH_3 .

Spectral Characterization of 4 and 5. NMR (^{31}P , ^{11}B , and ^1H). Spectral parameters are listed in Table III. Coupling constant data from ^1H spectra, using hetero- and homonuclear decoupling, were obtained. Coupling constants are as follows [referred to by notation used in Table III (J , Hz)]. For **4**: H_a-H_b (1.8), H_a-H_c (10.2), H_a-H_d (1.4), H_b-H_c (17.3), H_b-H_d (1.3), H_c-H_d (7.3), H_d-H_f (7.2), $P-H_a$ (2.0), $P-H_b$ (2.0), $P-H_c$ (4.2), $P-H_d$ (7.6). For **5**: H_a-H_d (2.7), H_d-H_f (7.4). **MS.** The most intense peak in the parent and five most intense ion envelopes are as follows [m/e (relative intensities)]. **4**: 88 (5), 74 (78), 57 (22), 45 (28), 41 (100), 39 (52). **5**: 86 (6), 72 (70), 69 (43), 57 (100), 45 (25), 39 (93). Weak ions at m/e 99, 132, and 174 in the spectrum of **4**, due to minor higher molecular weight species, were seen also.

Results and Discussion

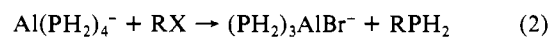
Synthesis and Characterization. Reactions between $\text{LiAl}(\text{PH}_2)_4$ (LAP) and the alkenyl and alkynyl halides $\text{CH}_2=\text{CHCH}_2\text{Cl}$, $\text{CH}_2=\text{CHCH}_2\text{Br}$, $\text{CH}_2=\text{CHCH}_2\text{CH}_2\text{Br}$, $\text{HC}\equiv\text{CCH}_2\text{Br}$, and $\text{CH}_2=\text{CHBr}$ were examined. Except in the LAP/ $\text{CH}_2=\text{CHBr}$

case, reaction occurs rapidly to form the corresponding alkenyl- or alkynylphosphine as

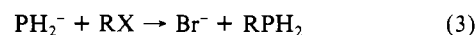


Yields of the pure phosphines typically are 60–75%. The yield of **1** is greater than reported⁴ or determined independently by us for the $\text{NaPH}_2/\text{CH}_2=\text{CHCH}_2\text{Cl}$ reaction. Isolated yields depend largely upon the degree of difficulty involved in product purification. Since the chloride reactants are close and slightly higher in volatility than the product phosphines, chlorides are less desirable than bromides for use in these syntheses. For example, $\text{CH}_2=\text{CHCH}_2\text{Cl}/\text{CH}_2=\text{CHCH}_2\text{PH}_2$ mixtures require repeated tedious high-vacuum column distillation¹⁰ for their complete separation. In contrast, $\text{CH}_2=\text{CHCH}_2\text{Br}/\text{CH}_2=\text{CHCH}_2\text{PH}_2$ mixtures are separable in one or two distillation steps.

Although LAP has been used extensively for the synthesis of silyl-, germyl-, and stannylphosphines,^{5–8} the mechanism of phosphination has not been studied in detail. An indication of the mechanism is obtained from comparison of the LAP/ $\text{CH}_2=\text{CHBr}$ reaction to reactions of LAP with CH_3I ,¹³ $\text{CH}_2=\text{CHCH}_2\text{X}$ ($\text{X} = \text{Cl}, \text{Br}$), $\text{CH}_2=\text{CHCH}_2\text{CH}_2\text{Br}$, or $\text{HC}\equiv\text{CCH}_2\text{Br}$. No phosphination of $\text{CH}_2=\text{CHBr}$ is observed even after 2.5 h at 25 °C. In contrast, the other halides react at temperatures as low as -30 °C. Since all reaction systems involved a common solvent, triglyme, the observed reactivity differences can be ascribed to differences in the halides. Since vinyl halides are known to be unreactive toward nucleophilic substitution,¹⁴ it is possible that LAP phosphinations are nucleophilic substitution processes. The halide displacement might involve complex aluminum phosphinide species [e.g., $\text{Al}(\text{PH}_2)_4^-$] as



A less likely process could involve free phosphinide ions (PH_2^-):



Further study of the LAP phosphination reactions are necessary in order to elucidate their mechanisms completely.

The advantages of LAP phosphinations lie in the mild reaction conditions required and the high-yield formation of single isomers; e.g., in the preparation of $\text{HC}\equiv\text{CCH}_2\text{PH}_2$, the isolated isomer predominated. In contrast, Hewertson et al. in studies of the $\text{Ph}_2\text{P}^-/\text{CH}\equiv\text{CCH}_2\text{Br}$ reaction report formation of $\text{CH}_2=\text{C}=\text{CHPPh}_2$ and $\text{CH}_3\text{C}=\text{CPPH}_2$ in addition to $\text{CH}\equiv\text{CCH}_2\text{PPh}_2$.¹⁵ They attributed this to base-catalyzed rearrangement of the 3-phosphino-1-propynyl isomer [$\text{CH}\equiv\text{CCH}_2\text{PPh}_2$]. The near absence of such isomerization reactions in the LAP systems is perhaps indicative of the low basicity of the LAP reagent.

Characterization of the new phosphines 1–3 is based on a combination of spectral, elemental analytical, and vapor tension data. In all cases the mass spectra showed parent ions, i.e. at m/e 74, 88, and 72 for $\text{CH}_2=\text{CHCH}_2\text{PH}_2$, $\text{CH}_2=\text{CHCH}_2\text{CH}_2\text{PH}_2$, and $\text{HC}\equiv\text{CCH}_2\text{PH}_2$, respectively. For $\text{CH}_2=\text{CHCH}_2\text{PH}_2$, the parent ion is also the most intense (base) peak. Fragmentation patterns are as expected; intense ions occur at m/e 41, 55, and 39, due to allyl (C_3H_7^+), butenyl (C_4H_7^+), and propargyl (C_3H_3^+) cations from $\text{CH}_2=\text{CHCH}_2\text{PH}_2$, $\text{HC}\equiv\text{CCH}_2\text{PH}_2$, and $\text{CH}_2=\text{CHCH}_2\text{CH}_2\text{PH}_2$, respectively.

The infrared spectra for 1–3 are summarized in Table I. In all three cases, strong P–H stretching absorptions occur in the 2290–2303- cm^{-1} range.^{16,17} Characteristic olefinic C–H and

(13) Shay, R. H.; Norman, A. D., unpublished data.

(14) March, J. *Advanced Organic Chemistry*, 3rd ed.; Wiley-Interscience: New York, 1985.

(15) Hewertson, W.; Taylor, I. C.; Trippett, S. *J. Chem. Soc. C* **1970**, 1835.

(16) Silverstein, R. M.; Bassler, G. C.; Morrill, T. C. *Spectrophotometric Identification of Organic Compounds*; Wiley: New York, 1974.

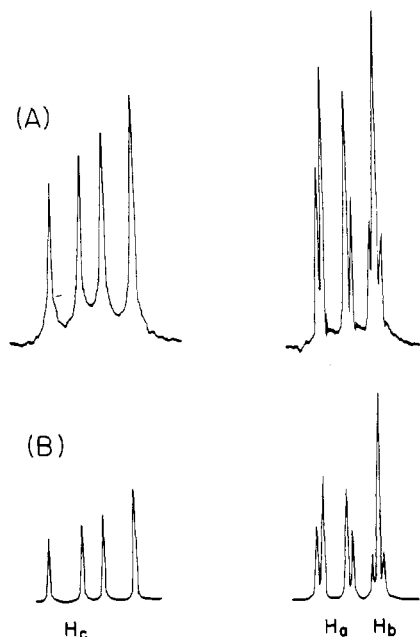


Figure 1. Observed (A) and calculated (B) 100-MHz ^1H NMR H_a , H_b , and H_c spectral resonances of $\text{CH}_2=\text{CHCH}_2\text{PH}_2$ when ^{31}P and $^1\text{H}(\text{CH}_2)$ decoupled.

saturated C—H stretching modes are seen in **1** and **2** at 3090 and 2984–2916 cm^{-1} . In addition, characteristic C=C bond absorptions at 1633 and 1642–1648 cm^{-1} in **1** and **2** occur.^{16,17} Absorptions at 3335, 2933, and 2129 cm^{-1} , characteristic of acetylenic C—H, saturated C—H, and C=C bond stretching modes, are seen.

^{31}P and ^{13}C NMR spectral parameters for $\text{CH}_2=\text{CHCH}_2\text{PH}_2$, $\text{CH}_2=\text{CHCH}_2\text{CH}_2\text{PH}_2$, and $\text{HC}\equiv\text{CCH}_2\text{PH}_2$, are given in Table II. Spectral assignments are based on resonance multiplicity patterns¹⁸ and correlations with analogous organophosphines.^{12,20} The ^{31}P NMR spectra of **1–3** show 1:2:1 triplets (singlets upon ^1H decoupling) from the PH_2 groups with $^1J(\text{P-H})$ values in the range expected. Similarly, the ^{13}C NMR resonances are readily assigned because of the close similarity between the phosphine spectra and those of analogue compounds, e.g. $\text{CH}_2=\text{CHCH}_2\text{PH}_2$ with $\text{CH}_2=\text{CCH}_2\text{X}$ ($\text{X} = \text{Cl}, \text{Br}, \text{CN}$),¹⁹ $\text{CH}_2=\text{CHCH}_2\text{CH}_2\text{PH}_2$ with $\text{CH}_2=\text{CHCH}_2\text{PH}_2$ and $(\text{CH}_2=\text{CHCH}_2\text{CH}_2)_3\text{P}$,²⁰ and $\text{HC}\equiv\text{CCH}_2\text{PH}_2$ with $\text{HC}\equiv\text{CCH}_2\text{Br}$. In all cases, the resonances fall in regions normally assigned to $=\text{CH}_2$, $\equiv\text{CH}$, $-\text{CH}_2-$, or $\equiv\text{C}$ -type carbon atoms.²¹

Proton NMR spectra of the primary phosphines, especially **1** and **2**, are more complex. The spectrum of $\text{CH}_2=\text{CHCH}_2\text{PH}_2$ (**1**) was analyzed in detail through use of homo- and heteronuclear decoupling and spectral simulation techniques.¹⁸ Spectral parameters and assignments are given in Table II. The spectrum exhibits the five resonances expected for a $\text{ABCD}_2\text{E}_2\text{X}$ ($\text{X} = \text{P}$ nucleus) spin system,¹⁸ although precise definition of chemical shifts required spin-decoupling techniques. Heteronuclear [$^1\text{H}\{^{31}\text{P}\}$] and simultaneous homonuclear [$^1\text{H}\{^1\text{H}\}$] spin decoupling of CH_2 protons reduces the system to an ABC spin pattern for protons H_a , H_b , and H_c (Figure 1). First-order analysis of this allows determination of the $^3J(\text{H}_b-\text{H}_c)$, $^3J(\text{H}_a-\text{H}_c)$, and $^2J(\text{H}_a-\text{H}_b)$ couplings and, by analogy with other $\text{CH}_2=\text{CHCH}_2\text{X}$ compounds,^{20,22} allows assignment of the H_c , H_b , and H_a protons at

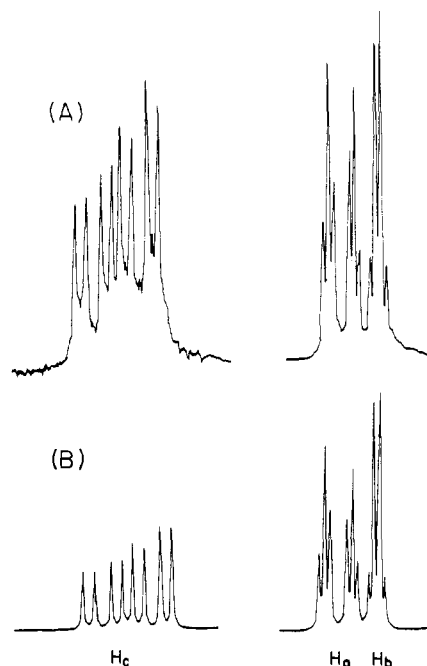


Figure 2. Observed (A) and calculated (B) 100-MHz ^1H NMR H_a , H_b , and H_c spectral resonances of $\text{CH}_2=\text{CHCH}_2\text{PH}_2$ when $^1\text{H}(\text{CH}_2)$ decoupled.

δ 5.09, 4.96, and 4.90, respectively. The spectrum of this region calculated by using the NMRCAL spectral simulation program and the above derived parameters (shown in Figure 1) is in close agreement with the observed spectrum. The spectrum with only homonuclear decoupling (CH_2 -decoupled), shows an ABCX pattern and demonstrates the added complexity that arises from introduction of the ^{31}P nucleus (Figure 2). From this spectrum, the couplings to phosphorus, $^3J(\text{P}-\text{H}_c)$ and $^4J(\text{P}-\text{H}_a)$ [and $^4J(\text{P}-\text{H}_b)$] of 4.2 and 2.0 Hz, are obtained. Assignment of chemical shifts is based on comparison of the spectrum of **1** with those of other $\text{CH}_2=\text{CHCH}_2\text{X}$ ($\text{X} = \text{H}, \text{Cl}, \text{Br}$) compounds. The doublet of doublets at δ 5.90 [$^3J(\text{H}_a-\text{H}_c) = 17.3$ Hz] is closely similar to that seen in $\text{CH}_2=\text{CHCH}_3$,²² and hence it is assigned to the H_c atom of $\text{CH}_2=\text{CHCH}_2\text{PH}_2$. An increasingly complex spectral pattern is observed when only the ^{31}P nucleus is decoupled. The resulting ABCD_2E_2 pattern and the completely undecoupled $\text{ABCD}_2\text{E}_2\text{X}$ spectrum can be closely simulated, providing further conformation for the overall spectral analysis. Closer agreement between the observed and calculated spectra may be possible with more sophisticated simulation methods, i.e. those in which more than six spins and variable line widths can be included.²³

Assignments of the ^1H NMR spectra of $\text{CH}_2=\text{CHCH}_2\text{CH}_2\text{PH}_2$ and $\text{HC}\equiv\text{CCH}_2\text{PH}_2$ are based on spectral multiplicity data and comparison of their spectra with those of known compounds. A detailed analysis of the $\text{CH}_2=\text{CHCH}_2\text{CH}_2\text{PH}_2$ spectrum was not carried out because of the limitations of the available NMRCAL spectral simulation program. However, similar to $(\text{CH}_2=\text{CHCH}_2\text{CH}_2)_3\text{P}$,²⁰ $\text{CH}_2=\text{CHCH}_2\text{CH}_2\text{PH}_2$ shows olefinic resonances at δ 4.9 (H_a and H_b) and δ 5.7 (H_c). An apparent quintet at δ 2.1 (area 2) is assigned to the methylene protons β to phosphorus (H_d), and a complex resonance at δ 1.4 (area 3) arises from the α - CH_2 proton (H_e).

Vapor pressure vs. temperature data for $\text{CH}_2=\text{CHCH}_2\text{PH}_2$, $\text{CH}_2=\text{CHCH}_2\text{CH}_2\text{PH}_2$, and $\text{HC}\equiv\text{CCH}_2\text{PH}_2$ were obtained in the temperature ranges -63.5 to 0.0 , -21.0 to $+37.5$, and -45.0 to 0.0 $^\circ\text{C}$, respectively. In all cases normal boiling points and

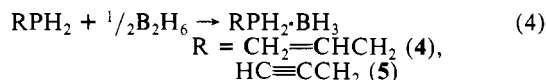
- (17) Thomas, L. C. *Interpretation of the Infrared Spectra of Organophosphorus Compounds*; Heyden and Sons: London, 1974.
 (18) Abrahams, R. A. *Analysis of High Resolution NMR Spectra*; Elsevier: Amsterdam, 1974.
 (19) Johnson, L. F.; Jankowski, W. C. *Carbon-13 NMR Spectra*; Wiley: New York, 1972.
 (20) Clark, P. W.; Curtis, J. L. S.; Garrou, P. E.; Hartwell, G. E. *Can. J. Chem.* **1974**, *52*, 1714.
 (21) (a) Levy, G. C.; Nelson, G. L. *Carbon-13 NMR Spectra of Organic Chemists*; Wiley-Interscience: New York, 1972. (b) Mann, B. E. *J. Chem. Soc., Perkin Trans. 2* **1972**, 30.

- (22) (a) Bothner-By, A. A.; Naar-Colin, C. *J. Am. Chem. Soc.* **1961**, *83*, 231. (b) Bockerman, G. N.; Parry, R. W. *Inorg. Nucl. Chem. Lett.* **1976**, *12*, 65. (c) Falardeau, E. R.; Morse, K. W.; Morse, J. G. *Inorg. Chem.* **1975**, *14*, 1239.
 (23) Castellano, S.; Bothner-By, A. A. *J. Chem. Phys.* **1964**, *41*, 3863.
 (24) Lewis, G. N.; Randall, M. *Thermodynamics*, 2nd ed.; McGraw-Hill: New York, 1961.

entropies of vaporization (ΔS_{vap}) are observed. The ΔS_{vap} values range from 95.4 J/(mol·deg) for $\text{CH}_2=\text{CHCH}_2\text{PH}_2$ to 110.0 J/(mol·deg) for $\text{HC}\equiv\text{CCH}_2\text{PH}_2$. The higher value for $\text{HC}\equiv\text{CCH}_2\text{PH}_2$ might indicate a slightly higher degree of intermolecular association in the vapor phase for the $\text{HC}\equiv\text{CCH}_2\text{PH}_2$ than for the alkenyl derivatives (**1** or **2**).

Borane Coordination. The coordination properties of alkenyl- and alkynylphosphines toward B_2H_6 is of interest to compare with organophosphine-borane coordination chemistry observed previously.²⁵⁻²⁷ Because of its relatively strong Lewis acidity toward "soft" donors, B_2H_6 generally reacts with phosphines to form BH_3 adducts. However, with the alkenyl- and alkynylphosphines the possibility exists that coordination might occur also or preferentially at the C=C or C≡C bond sites, since BH_3 units are known to add efficiently across these bonds, e.g. as occurs in hydroboration.²⁸

Reactions of $\text{CH}_2=\text{CHCH}_2\text{PH}_2$ and $\text{HC}\equiv\text{CCH}_2\text{PH}_2$ with excess B_2H_6 occur smoothly at -78 to -45 °C to form 1:1 phosphine: BH_3 adducts **4** and **5** as



Only at longer reaction times and at higher temperatures does further reaction of B_2H_6 occur, presumably with reaction at the C=C or C≡C bonds in the adducts. Mass spectral data show that **4** and **5** remain associated in the gas phase; **4** and **5** exhibit parent ions at m/e 88 and 86, respectively. **4** also shows minor spectral peaks up to m/e 174, which likely arise either from traces of decomposition in the spectrometer inlet or from oligomerization of **4** in the gas phase.

That BH_3 coordination in **4** and **5** occurs at phosphorus and not at the C=C or C≡C bonds is clear from the NMR spectral data. The ^{11}B NMR spectra exhibit quartets (^{11}B - ^1H coupling) of doublets (^{11}B - ^{31}P coupling) at δ -42.4 and -41.3, respectively. Coupling of the ^{11}B nucleus to the PH_2 protons is small and not measurable. Chemical shifts and coupling constants agree closely with those reported previously for primary phosphine-boranes.^{26,27} The ^{31}P NMR spectra consist of triplets [$J(\text{P}-\text{H})$] at δ -48.2 and -41.9, in which each spectral member is strongly broadened as is expected for PH_2 groups coupled weakly to BH_3 groups. The $^1J(\text{P}-\text{H})$ couplings in **4** and **5** are nearly twice what they are in **1** and **2**, again a situation reported earlier by Cowley and Damasco.²⁵ Also, borane coordination results in large downfield coordination shifts (84.4 ppm for **4**, 88.7 ppm for **5**) as is typically observed in borane or transition-metal complexes.²⁹

The ^1H NMR spectra of **4** and **5** are assigned by using heteronuclear (^{11}B and ^{31}P) spin decoupling and by comparison of the spectra with those for **1** and **2**. Assignments are given in Table III, although proton coupling constants were not examined as extensively as in **1**. The $\text{CH}_2=$, $=\text{CH}$ -, and $-\text{CH}_2$ - protons of **4** and the $\equiv\text{CH}$ and $-\text{CH}_2$ - protons of **5** show little variance from their positions in **1** and **2**. The BH proton resonances, which undecoupled are quartets (with minor septets due to ^{10}B coupling) in the undecoupled spectra, collapse to doublets [$^2J(\text{H}-\text{P})$] of triplets [$^3J(\text{H}-\text{H})$] upon ^{11}B decoupling. The PH_2 protons are doublets of apparent sextets as a result of fortuitous peak overlap that results from coupling to the BH_3 and $-\text{CH}_2$ - protons. Since PH_2 proton coupling to the ^{11}B nucleus is small, it is only weakly evident. Assignment of the "sextet" peaks is substantiated by the absence of a ^{11}B -decoupling effect and by the $^1\text{H}\{^{31}\text{P}\}$ spectra, where the $-\text{CH}_2$ - resonances are single triplets [$^3J(\text{H}_a-\text{H}_\beta)$]. In **5**, a $^4J(\text{H}_a-\text{H}_\gamma)$ of 3.0 Hz involving coupling of PH_2 protons to the H_a proton is also seen.

Complexes **4** and **5** are thermally unstable with respect to oligomerization/polymerization. Above 25 °C, **4** decomposes slowly to an oil that later becomes an intractable solid. **5** decomposes above 0 °C to form a resinous product along with some $\text{HC}\equiv\text{CCH}_2\text{PH}_2$ and $\text{PH}_3\cdot\text{BH}_3$.³⁰ Similar behavior has been reported for the complex $\text{CH}_2=\text{CHCH}_2\text{PH}(\text{CH}_3)\cdot\text{BH}_3$.³¹ Although details of these oligomerization/polymerization reactions are not known, they could be of sufficient interest to warrant further studies.

Acknowledgment. Support of this work by National Science Foundation grants (CHE-7909497 and CHE-8312856) and the Colorado Advanced Materials Institute is gratefully expressed.

Registry No. **1**, 81637-99-2; **2**, 114596-01-9; **3**, 114596-02-0; **4**, 114596-03-1; **5**, 114596-04-2; $\text{CH}_2=\text{CHCH}_2\text{Cl}$, 107-05-1; $\text{CH}_2=\text{CHC}-\text{H}_2\text{Br}$, 106-95-6; $\text{CH}_2=\text{CHCH}_2\text{CH}_2\text{Br}$, 5162-44-7; $\text{HC}\equiv\text{CCH}_2\text{Br}$, 106-96-7; $\text{LiAl}(\text{PH}_2)_4$, 25248-80-0; $\text{CH}_2=\text{CHBr}$, 593-60-2.

(30) Rudolph, R. W.; Parry, R. W.; Farran, C. F. *Inorg. Chem.* **1966**, *5*, 723.

(31) Wagner, R. I.; Wilson, C. O. *Inorg. Chem.* **1966**, *5*, 1009.

Contribution from the School of Chemical Sciences,
University of East Anglia, Norwich NR4 7TJ, England

Equilibrium Dissociation of Tetrakis(acetato)dichromium(II) in Acetic Acid/Water Media

L. M. Wilson and R. D. Cannon*

Received November 19, 1987

Chromium(II) acetate is predominantly dimeric in both water and acetic acid solutions, as shown by the red-brown color and similarity of absorption spectra¹ and by measurements of the dissociation constant in aqueous media.^{2,3} Copper(II) acetate has the dimeric structure in the solid state and in nonpolar solvents, but in water it is fully dissociated into monomeric complexes.⁴ In acetic acid solution, however, the dissociation constants of the copper dimer have been measured.⁵ Evidently the copper-copper bond is weaker than the chromium-chromium bond, and we have attempted previously to quantify the difference, by estimating the copper dissociation constant in aqueous solution.⁴ In order to provide a more direct comparison and to interpret more fully the kinetics of redox reactions in acetic acid media,⁶ we have now determined the chromium dissociation constant in acetic acid media with varying water content. Care was taken to control the water activity and to allow for side oxidation of chromium(II) by analyzing the chromium(II) concentrations in situ.

Experimental Section

Chromium(II) acetate hydrate, $\text{Cr}_2(\text{OAc})_4\cdot 2\text{H}_2\text{O}$, was prepared as before^{3a} and dried under flowing nitrogen. Acetic acid was dried by refluxing with $\text{B}(\text{OAc})_3$ ⁷ and redistilled. Water content of solutions was determined by the Karl Fischer method⁸ using a visual or electrometric end point as appropriate. Stock solutions of chromium(II) acetate in acetic acid were mixed with further acetic acid, and with water, in glass spectrophotometric cells modified with a screw top and a PTFE-silicone rubber septum. All solutions were dispersed under nitrogen from the

(25) Wiberg, E.; Amberger, E. *Hydrides of the Elements of Main Groups I-IV*; Elsevier: Amsterdam, 1971.

(26) Cowley, A. H.; Damasco, M. C. *J. Am. Chem. Soc.* **1971**, *93*, 6815.

(27) (a) Rudolph, R. W.; Schultz, C. W. *J. Am. Chem. Soc.* **1971**, *93*, 6821. (b) Falardeu, E. R.; Morse, K. W.; Morse, J. G. *Inorg. Chem.* **1974**, *13*, 2333.

(28) Brown, H. C. *Boranes in Organic Chemistry*; Cornell University Press: Ithaca, NY, 1972.

(29) Klanberg, F.; Muetterties, E. L. *J. Am. Chem. Soc.* **1968**, *90*, 3296.

(1) Furlani, C. *Gazz. Chim. Ital.* **1951**, *87*, 885.

(2) Cannon, R. D. *J. Chem. Soc. A* **1968**, 1098. Cannon, R. D.; Stillman, J. S. *Inorg. Chem.* **1975**, *14*, 2202.

(3) (a) Cannon, R. D.; Gholami, M. J. *J. Chem. Soc., Dalton Trans.* **1976**, 1574. (b) Cannon, R. D.; Gholami, M. J. *Bull. Chem. Soc. Jpn.* **1982**, *55*, 594.

(4) Cannon, R. D. *Inorg. Chem.* **1981**, *20*, 2341 and references cited therein.

(5) Cheng, A. J. A.; Howald, R. A. *Inorg. Chem.* **1968**, *7*, 2100.

(6) Wilson, L. M.; Cannon, R. D. *Inorg. Chem.* **1985**, *24*, 4366.

(7) Eichelberger, W. E.; La Mer, V. K. *J. Am. Chem. Soc.* **1933**, *55*, 3633.

(8) Smith, D. M.; Bryant, N. M.; Mitchell, J. J. *J. Am. Chem. Soc.* **1939**, *61*, 2407.